Proceedings of the ASME 2018
Dynamic Systems and Control Conference
DSCC2018
September 30-October 3, 2018, Atlanta, Georgia, USA

DSCC2018-9226

DESIGN AND EVALUATION OF A PROPORTIONAL MYOELECTRIC CONTROLLER FOR HIP EXOSKELETONS DURING WALKING

Hsiang Hsu, Inseung Kang, Aaron J Young PhD
Department of Mechanical Engineering
Georgia Institute of Technology
Atlanta, GA 30332, USA
Email: hhsu24@gatech.edu

ABSTRACT

The purpose of this study was to explore the effectiveness of a neural controller for a single-joint bilateral hip exoskeleton. The device provides mechanical torque in the sagittal plane and uses series elastic actuators for feedback control. The system consists of three control layers: (1) a high-level controller that estimates the current gait phase, (2) a mid-level controller that converts the electromyography (EMG) signals to desired exoskeleton torques, and (3) a low-level controller that ensures the output torque matches the commanded torque. To evaluate the effectiveness of the proportional EMG controller, one able-body subject walked with the exoskeleton under 3 assistance conditions: (1) a baseline proportional gain condition ($\times G$), (2) a double proportional gain condition ($\times 2G$) for faster scaling, and (3) an on/off set value torque assistance (SV). The third condition provides the same net mechanical power as the baseline ($\times G$) condition to compare whether proportional scaling of the hip torque was significant. The subject's hip-joint kinematics, metabolic rate, and muscle activities were collected as outcome measurements. In summary, the EMG controller could generate seamless torque to the user with a response time of 80 ms. The $\times 2G$ condition resulted in a 23.3% EMG activity reduction while SV condition reduced the metabolic rate by 8.1%. Interestingly, the largest EMG reduction condition ($\times 2G$) did not result in largest metabolic reduction (SV). Our preliminary findings suggest that the proportional scaling of the hip torque may not be the most important parameter to minimize metabolic cost.

INTRODUCTION

The global exoskeleton market is expected to exceed 3.5 billion by 2025 and offers alternative solutions to numerous fields such as work-injury prevention, muscle rehabilitation, and human augmentation [1]. Existing commercial exoskeletons such as Indego [2], Ekso [3], and ReWalk [4] as well as many research exoskeletons [5-8] often use mechanical sensors to interpret user's intention and command the robot accordingly. Since mechanical sensors usually lag behind the user's movement, the metabolic benefits from such control strategies were often marginal. Moreover, mechanical controllers often have difficulty adapting to disturbances such as change of speed or altered walking patterns. As a result, exoskeletons are mainly effective only in controlled environments such as constant speed treadmill walking.

Electromyography (EMG) readings of muscles are highly correlated to the user's intention as they contain information about the user's muscle movements. The inherent electro-mechanical delay of the EMG signals means the signals would be generated about 30-100 ms before muscle contractions [9]. Hence, by interpreting the EMG signals, the exoskeleton would be able to determine the user's intention and generate assistance before the intended movement. Such control strategies had been proposed and implemented as alternative control strategies by several groups [10-12]. While extremely popular and well-studied in upper-limb exoskeletons, the usability of EMG controller on lower body exoskeletons has not been explored by many research groups [13-15]. HAL [16] is the only commercially available lower-limb exoskeleton that utilizes EMG as part of its control algorithm.

Previous studies have shown that while the hip and ankle joints are major mechanical energy drivers for level ground walking, the hip may be less efficient at generating mechanical power than the ankle due to anatomical muscle structures [17]. Therefore, our lab has developed an active hip exoskeleton that provides hip flexion and extension torque to the user. A proportional myoelectric controller was developed to explore the effectiveness of the neural controller. The controller proportionally scales the EMG signal from a hip flexor (rectus femoris) or extensor (gluteus maximus) to output a torque command to the exoskeleton. One able-bodied subject walked on a treadmill with three different EMG-based assistance profiles. The first condition served as a baseline with a constant gain ($\times G$), where torque command equaled to the EMG reading multiplied by the gain. The second condition had a double gain ($\times 2G$) where the torque would scale twice as fast as the baseline condition. The third condition had an on/off set value (SV) torque command. The constant torque value was pre-defined, so the exoskeleton would provide the same amount of power for both $\times G$ and SV condition. This allowed for a direct comparison of whether proportional scaling was important or not. Outcome measurements of EMG activities and metabolic cost were used for validation.

1 CONTROLLER DESIGN

1.1 Powered Hip Exoskeleton

Figure 1 shows the bilateral hip exoskeleton used for the proposed study. The motors can provide power assistance in both hip flexion and extension (total of 130°) with an additional passive joint in the frontal plane, which allows the user to freely circumduct the hip (total of 30°). The device was designed to match the biological hip torque during walking. Therefore, it can provide 60 Nm of peak torque and 30 Nm of continuous torque with an angular velocity of 180°/sec. For high fidelity closed-loop control, the exoskeleton utilizes a set of series elastic actuators to measure and control torque. Custom interfaces within the device such as thigh shells, a pelvic band, and backpack straps allowed the device to effectively assist the user through attachment points.

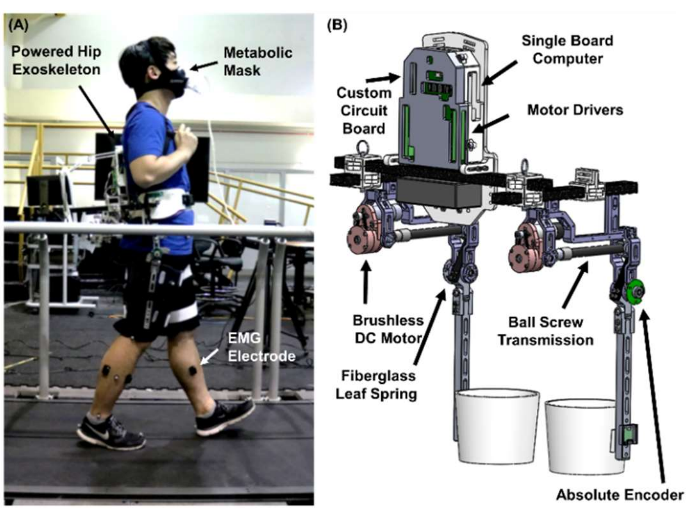

Figure 1. Overview of the powered hip exoskeleton (a) Example of a subject walking on a treadmill with the exoskeleton (b) Key components of the exoskeleton illustrated with detailed CAD design

1.2 Device Components

Key components used in each series elastic actuator unit are: a 200W brushless DC motor (EC30, Maxon Motor, Switzerland), a ball-screw transmission (Thomson Linear Motion, USA), and a fiberglass leaf spring (Gordon Composite, USA). To measure the spring deflection, a set of strain gauges (Omega Engineering, USA) were attached in a full Wheatstone bridge configuration. Each of the motors was controlled by a servo motor driver (ESCON 50/5 Module, Maxon Motor, USA) operating with a low-level current control. A 14-bit absolute magnetic encoder (Orbis, Renishaw, UK) was placed along the output hip joint to measure the hip joint kinematics. Additionally, a set of force sensitive resistors (FSRs) were attached to the user's heels for gait phase estimation. All on-board sensors and actuators were processed with a single board computer (myRIO, National Instruments, USA), which was housed in the backpack unit. Lastly, 4 channels of surface electromyography sensors (DataLINK, Biometrics Ltd, UK) were attached to the user's legs to measure muscle activities.

1.3 Exoskeleton Control Architecture

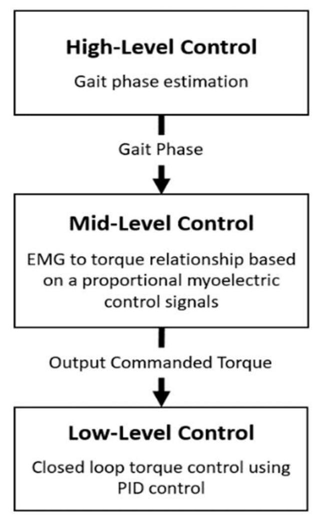

Figure 2. Control architecture of the exoskeleton. High-level controller sends gait phase information to mid-level controller which generates proportional torque commands based on muscle activation. The low-level controller performs closed loop torque control using the SEAs.

The entire exoskeleton control has three distinct tiers where different control strategies can be implemented inside of each layer (Fig 2). The high-level control layer uses FSRs as event markers and outputs a continuous gait phase estimation. It divides the time since last heel strike by the average stride time as the % gait cycle. The average stride time is computed from the previous 5 strides. The mid-level myoelectric control layer takes EMG signals and generates corresponding torque commands based on the current gait phase information received from the high-level controller. The low-level controller then uses strain gauges to determine the applied torque and matches the desired torque via a PD controller.

1.4 Proportional Myoelectric Controller Design

The mid-level control layer often dictates how the exoskeleton interacts with the user using certain dynamic equations. Admittance control, trajectory-based control, and biological torque control are some of the different mid-level control strategies available. We propose a proportional EMG controller which uses one hip flexor and one extensor as main control signals.

Rectus femoris (RF) and gluteus maximus (GM) are two of the main hip flexor and extensor muscles. One EMG electrode was attached to RF for exoskeleton flexion command while another one was attached to GM for extension. One of the main challenges for EMG controller implementation is deciding which channel to use as the input throughout the gait cycle. During walking, both RF and GM could co-contract and the controller needs to select the proper muscle signal as its torque input. The hip is primarily extending during late swing to early stance. Hence, a conservative discard approach was implemented where the controller would disregard the hip flexor readings during 80% – 30% of the gait cycle (and vice versa for hip extensor).

The single board computer sampled the raw EMG signal at 1 kHz to minimize aliasing. To avoid potential phase shift, we used a simple root mean square (RMS) filter with a minimal window size of 10 ms. When the EMG reading passed a preset threshold, the commanded exoskeleton torque is scaled proportionally with the EMG reading by a gain constant ($\times G$ or $\times 2G$). This generated torque command would be discarded if the gait phase did not meet the criteria mentioned above. When the commanded torque was zero, the exoskeleton passively followed the user's movement. The controller limited the maximum allowable torque to 20% biological hip torque for safety considerations [18].

2 CONTROLLER VALIDATION

The proportional EMG controller validation was performed through human subject testing approved by the Georgia Institute of Technology Institutional Review Board. One able-bodied subject (27 years old, male) was recruited and signed the written consent form prior to the experiment.

2.1 Methods

The subject completed a prior training session where he walked in the exoskeleton for 5 minutes under each condition. On the data collection day, the experimenter attached four EMG electrodes to the subject: (1) right rectus femoris, (2) right gluteus maximus, (3) left rectus femoris, and (4) left gluteus maximus. The subject walked on a treadmill (TuffTread, USA) at 0.8 m/s while the experimenter tuned the subject-specific parameters such as EMG thresholds and gains. Once the controller parameters were tuned, the subject then put on the exoskeleton and walked. Three different assistance conditions (Fig 3) were applied to the user. The first condition had a baseline gain ($\times G$) where the assistance torque would scale proportionally to the EMG signal. The second condition had a doubled gain ($\times 2G$) where the assistance torque would scale twice as fast. This $\times$ 2G condition results in a larger and longer assistance profile than $\times$G condition. The last condition was an on/off set value (SV) assistance condition which would only turn on when the EMG threshold was reached. The predefined set value was computed by taking the RMS of the torque in $\times G$ condition and divided by assistance duration. This ensured the same amount of the net power was delivered in both $\times G$ and SV condition, with the proportionality being the independent variable. Data from the hip joint encoder, strain gauge, metabolic analysis system (TrueOne 2400, Parvo Medics, USA), and EMG signals were collected. Four 6-minute trials were conducted, including a standing metabolic condition. (Total of 24 minutes)

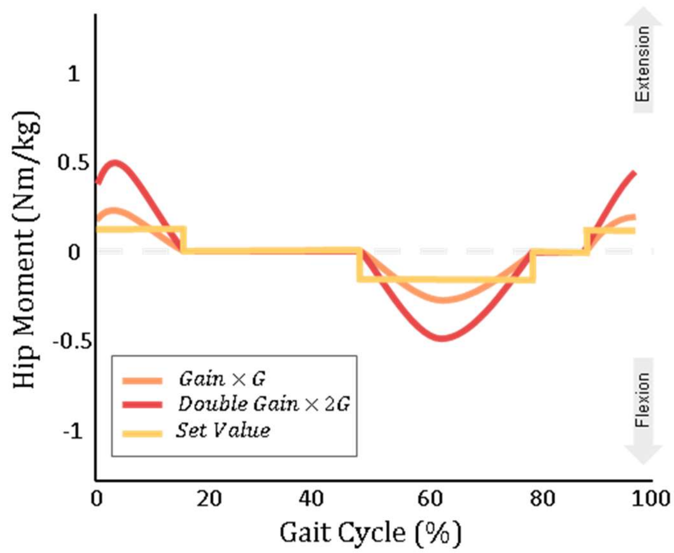

Figure 3. Three EMG-based exoskeleton assistance profiles: baseline gain (×G), double gain (×2G), and on/off set value assistance (SV). The ×G condition scaled the exoskeleton torque proportionally to the EMG signal. The ×2G condition scaled the torque twice faster than ×G condition. The SV condition provided a constant torque assistance.

2.2 Results

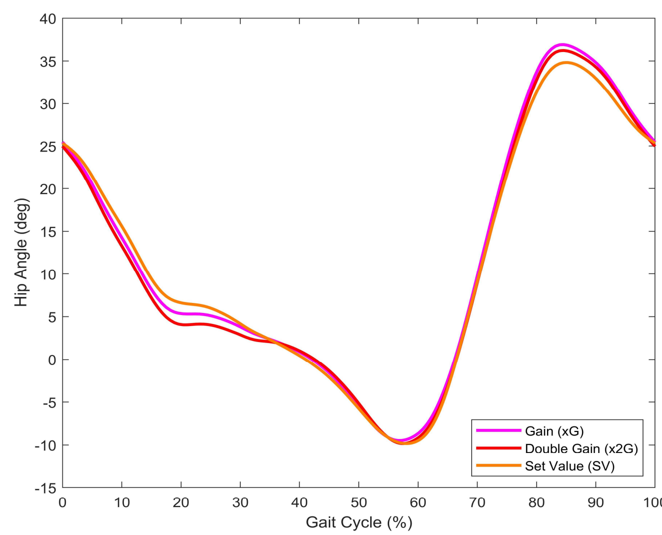

Figure 4. Hip joint kinematics across three assistance conditions. The hip joints agreed with the profile shown in literature with ×2G condition having the highest deviation due to assistance.

The hip joint kinematics for all three conditions agreed with those shown in the literature [19]. Yet, the slight variations highlighted the difference in assistance magnitude with $\times 2G$ showing the largest deviation (Fig 4). The mechanical delay between the commanded torque and applied torque was approximately 50ms. Combined with the RMS filter delay, the overall delay from the exoskeleton receiving EMG signals to applying torque to the user was around 80ms. Within the inherent 30 – 100 ms electro-mechanical delay range [9], our EMG controller could interpret and respond to the user's movements simultaneously, if not sooner than the actual muscle movements.

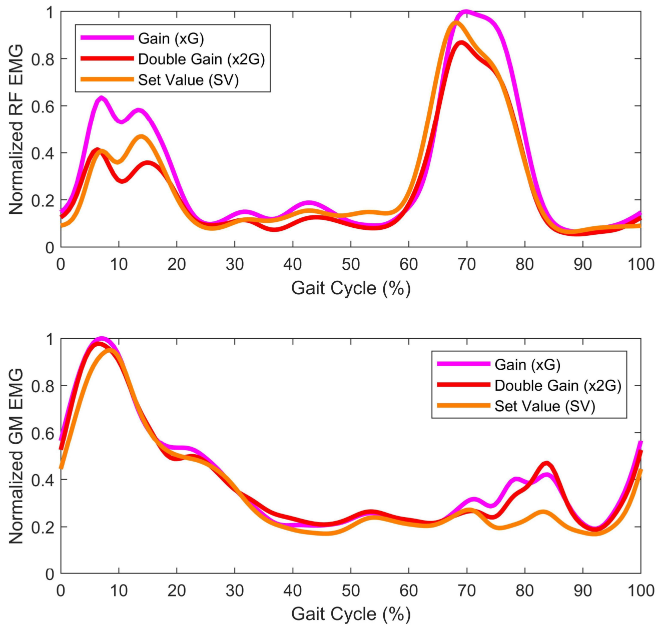

Figure 5. Normalized EMG activities across all three conditions with ×G as the baseline. The subject showed EMG activity reductions in both ×2G and ×SV conditions.

The last 3 minutes of the EMG data (Fig 5) were integrated to numerically represent muscle activations. Using $\times G$ as the baseline, Table 1 shows the percentage of EMG activity reduction for $\times 2G$ and SV conditions. For the $\times 2G$ condition, the hip flexor (RF) showed a 26.1% reduction while the hip extensor (GM) only had a 1.8% reduction. On the other hand, the SV condition reduced hip flexor and extensor activity by 11.5% and 11.8%, respectively. Intriguingly, the hip extensor benefited the most while the exoskeleton provided a constant flexion assistance during 70% - 90% of the gait cycle in SV condition.

Table 1. EMG activity reduction comparing to ×G condition

	$\boldsymbol{Flexion\ Diff}$ $\boldsymbol{from\ Gain(\times G)}$	$\boldsymbol{Extension\ Diff}$ $\boldsymbol{from\ Gain(\times G)}$
Gain (×G)	0%	0%
Double Gain (×2G)	−26.1%	−1.8%
Set Value (SV)	−11.5%	−11.8%

We also looked at the first and last minute of each trial's EMG data to examine the effect of adaptation [20]. For each condition and muscle, the first minute of the EMG signals were normalized as the baseline. Last minute's EMG activations were much lower than the first minute baselines (Fig 6). While hip flexor activity decreased 30.5% for $\times 2G$ condition, the hip extensor activity only dropped by 2.8%. The SV condition had the similar trend where the EMG decreased by 15.8% for flexor and 2.6% for extensor. The $\times G$ condition had even adaptations on both the hip flexor (14.5%) and the extensor (13.1%).

Table 2. Last min EMG adaptation comparing to the 1st min

	$\boldsymbol{Flexion\ Diff}$ $\boldsymbol{from\ 1^{st}\ min}$	$\boldsymbol{Extension\ Diff}$ $\boldsymbol{from\ 1^{st}\ min}$
Gain (×G)	−14.5 %	−13.1%
Double Gain (×2G)	−30.5%	−2.8%
Set Value (SV)	−15.9%	−2.6%

Of the 6 min trials, only the last 3 min of the metabolic data was used to ensure the subject reached metabolic steady-state. Using Brockway's equation with the recorded $\dot{V}O_2$ and $\dot{V}CO_2$, we computed the gross energy expenditure for each assistance condition [21]. We then subtracted the standing metabolic rate to calculate the net metabolic rates during walking (Table 3). With $\times G$ condition as baseline, $\times 2G$ condition had a 4.9% reduction whereas SV condition had an 8.1% reduction.

Table 3. Metabolic Outcome for each Assistance profile

	$\boldsymbol{Net\ Metabolic}$ $\boldsymbol{Rate\ (W/kg)}$	$\boldsymbol{Diff\ from}$ $\boldsymbol{the\ baseline}$
Gain (×G)	1.68	0%
Double Gain (×2G)	1.59	−4.9%
Set Value (SV)	1.54	−8.1%

3 DISCUSSION

The finding from this study demonstrates that the proportional EMG controller can reduce metabolic cost during walking. With simple RMS filtering, the exoskeleton successfully extracted and responded to the user's intentions within 100 ms. Compared to a mechanical controller, our controller allowed for smooth assistance and could adapt to disturbances on a stride-by-stride basis. Given more powerful computing and transmission units, it would be possible to align exoskeleton actuation with the muscles' biological force output.

Muscle adaptations occurred within the 6-minute walking trial throughout all 3 conditions (Fig 6). Since muscle activations are highly correlated to muscle contractions, lower EMG values

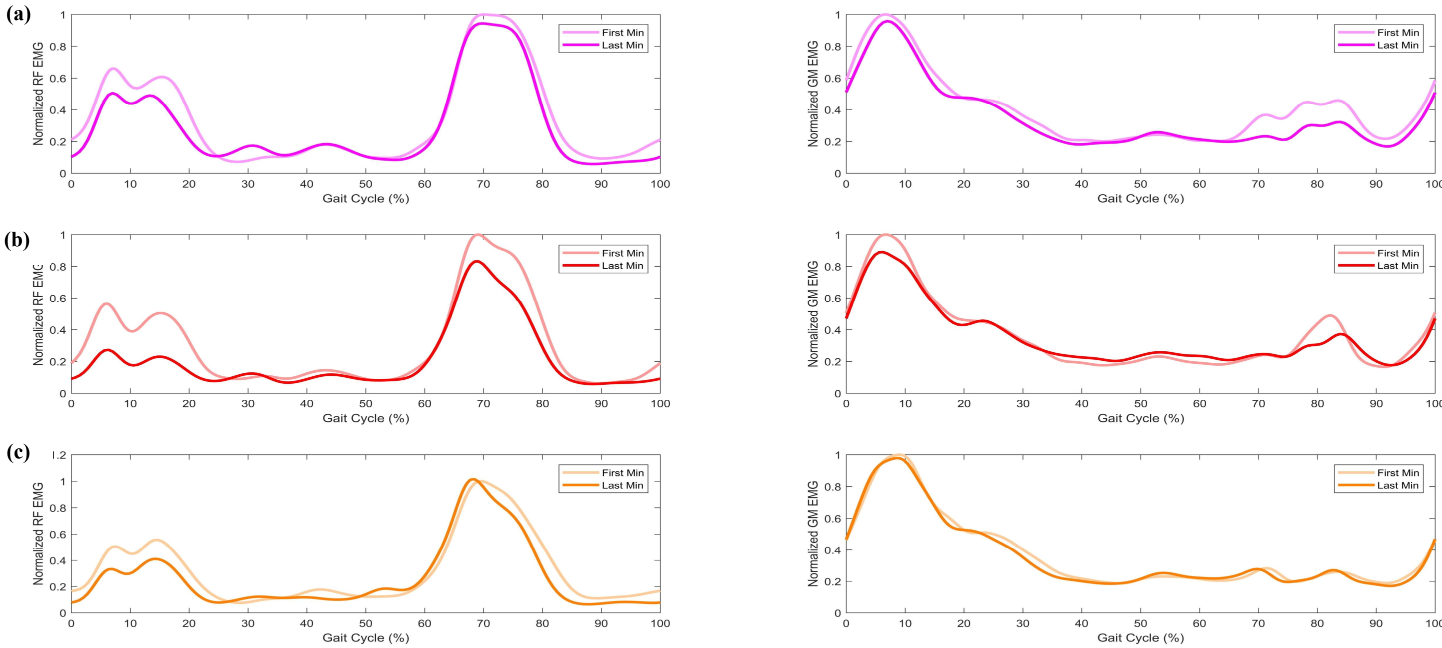

Figure 6. RMS values for hip flexor (left column) and extensor (right column) across gait cycle. Light lines represent the first min of the trial whereas dark lines represent the last min of the trial. (a) baseline gain ×G (b) double gain ×2G (c) on/off set value torque assistance (SV). The adaptations shown in all three conditions suggested the user was able to benefit from the exoskeleton assistance.

represents a reduced muscle intensity. This indicated that the subject did not have to work as hard with the EMG-based exoskeleton assistance. By comparing $\times 2G$ condition to the baseline, there was a 27.9% EMG reduction and a 4.9% metabolic reduction. The increased torque scaling allowed for the user to receive more mechanical power from the exoskeleton, and thus achieved a reduced metabolic rate. For the comparison whether proportional scaling was significant or not ($\times G$ vs SV), the subject showed a net 23.3% EMG reduction and an 8.1% decreased metabolic consumption. The results suggested a constant assistance profile might have better performance than a proportional assistance profile. The inter-condition comparisons suggested that the $\times 2G$ condition should perform the best with the highest EMG reduction (27.9%). However, the SV condition had the best overall metabolic performance despite having less EMG reduction (23.3%). Different from the asymmetric reduction in the $\times 2G$ condition, the symmetric EMG reduction in both the hip flexor and extensor in the SV condition may play a role in metabolic performance.

One major challenge for EMG controller is the controller robustness over time. Our proposed EMG controller relies heavily on a single muscle (RF/GM) signal for flexion/extension assistance. Over the long period of use, electrodes tend to shift due to sweat and movements. Even a slight displacement could result in drastic EMG signal changes [22]. Besides, the inherent variability could alter the subject's EMG signal from trial to trial as shown in previous study [23]. In our study, we used a discard approach to ignore the muscle signal during co-contraction. However, a different approach, such as summing both flexor and extensor signals, could be explored in future studies. Lastly, the proportional EMG controller requires precise and extensive parameter tuning for each subject. On the other hand, the SV condition only required threshold to be tuned, which makes it more ideal strategy for real-world implementation.

4 CONCLUSION

The purpose of this study was to design, implement, and evaluate a myoelectric controller on a hip exoskeleton. The EMG controller can provide seamless interactions with the user by synchronizing the exoskeleton torque to user muscle activity patterns. The controller's response time was about 80 ms and allowed for a smooth exoskeleton torque along the user's biological torque output. Three different EMG-based assistance profiles were investigated to understand the effect of torque scaling. We found muscle adaptations for all three conditions, suggesting that the EMG-based controller is an effective control algorithm. While the subject showed the most EMG reduction (27.9%) in $\times 2G$ condition, the best metabolic reduction (8.1%) occurred with the SV condition. The finding suggested the proportional scaling might not be the most important parameter in overall human performance. Further clinical testing and data collection will solidify the findings from our preliminary results.

ACKNOWLEDGEMENT

The authors thank Jevons Li and Ron Hong for helping with the data collection. We acknowledge Courtland Bivens and Michael Mayo at GTRI for their contributions and GTRI IRAD funding. Additionally, this work was funded by a seed grant through the Institute for Robotics and Intelligent Machines (IRIM) at Georgia Tech.

REFERENCES

[1] A. J. Young and D. P. Ferris, "State of the Art and Future Directions for Lower Limb Robotic Exoskeletons," (in

English), *Ieee Transactions on Neural Systems and Rehabilitation Engineering,* vol. 25, no. 2, pp. 171-182, Feb 2017.

[2] R. J. Farris, H. A. Quintero, S. A. Murray, K. H. Ha, C. Hartigan, and M. Goldfarb, "A preliminary assessment of legged mobility provided by a lower limb exoskeleton for persons with paraplegia," *IEEE Transactions on Neural Systems and Rehabilitation Engineering,* vol. 22, no. 3, pp. 482-490, 2014.

[3] S. A. Kolakowsky-Hayner, J. Crew, S. Moran, and A. Shah, "Safety and feasibility of using the EksoTM bionic exoskeleton to aid ambulation after spinal cord injury," *Journal of Spine,* 2013.

[4] G. Zeilig, H. Weingarden, M. Zwecker, I. Dudkiewicz, A. Bloch, and A. Esquenazi, "Safety and tolerance of the ReWalk™ exoskeleton suit for ambulation by people with complete spinal cord injury: A pilot study," *The Journal of Spinal Cord Medicine,* vol. 35, no. 2, pp. 101-96, 2012.

[5] A. B. Zoss, H. Kazerooni, and A. Chu, "Biomechanical design of the Berkeley lower extremity exoskeleton (BLEEX)," (in English), *Ieee-Asme Transactions on Mechatronics,* vol. 11, no. 2, pp. 128-138, Apr 2006.

[6] F. Giovacchini *et al.*, "A light-weight active orthosis for hip movement assistance," *Robotics and Autonomous Systems,* vol. 73, pp. 123-134, 2015/11/01/ 2015.

[7] K. Seo, J. Lee, Y. Lee, T. Ha, and Y. Shim, "Fully autonomous hip exoskeleton saves metabolic cost of walking," in *2016 IEEE International Conference on Robotics and Automation (ICRA)*, 2016, pp. 4628-4635.

[8] B. T. Quinlivan *et al.*, "Assistance magnitude versus metabolic cost reductions for a tethered multiarticular soft exosuit," *Science Robotics,* vol. 2, no. 2, 2017.

[9] H. Begovic, G.-Q. Zhou, T. Li, Y. Wang, and Y.-P. Zheng, "Detection of the electromechanical delay and its components during voluntary isometric contraction of the quadriceps femoris muscle," (in English), *Frontiers in Physiology,* Original Research vol. 5, no. 494, 2014-December-23 2014.

[10] J. Gancet *et al.*, "MINDWALKER: Going one step further with assistive lower limbs exoskeleton for SCI condition subjects," in *2012 4th IEEE RAS & EMBS International Conference on Biomedical Robotics and Biomechatronics (BioRob)*, 2012, pp. 1794-1800.

[11] K. Kiguchi, T. Tanaka, and T. Fukuda, "Neuro-fuzzy control of a robotic exoskeleton with EMG signals," *IEEE Transactions on Fuzzy Systems,* vol. 12, no. 4, pp. 481-490, 2004.

[12] T. Lenzi, S. M. M. D. Rossi, N. Vitiello, and M. C. Carrozza, "Intention-Based EMG Control for Powered Exoskeletons," *IEEE Transactions on Biomedical Engineering,* vol. 59, no. 8, pp. 2180-2190, 2012.

[13] D. P. Ferris and C. L. Lewis, "Robotic lower limb exoskeletons using proportional myoelectric control," in *2009 Annual International Conference of the IEEE Engineering in Medicine and Biology Society*, 2009, pp. 2119-2124.

[14] L. Grazi, S. Crea, A. Parri, R. Molino Lova, S. Micera, and N. Vitiello, "Gastrocnemius Myoelectric Control of a Robotic Hip Exoskeleton Can Reduce the User's Lower-Limb Muscle Activities at Push Off," (in English), *Frontiers in Neuroscience,* Original Research vol. 12, no. 71, 2018-February-14 2018.

[15] A. J. Young, H. Gannon, and D. P. Ferris, "A Biomechanical Comparison of Proportional Electromyography Control to Biological Torque Control Using a Powered Hip Exoskeleton," *Frontiers in Bioengineering and Biotechnology,* vol. 5, p. 37, 2017.

[16] H. Kawamoto, L. Suwoong, S. Kanbe, and Y. Sankai, "Power assist method for HAL-3 using EMG-based feedback controller," in *Systems, Man and Cybernetics, 2003. IEEE International Conference on*, 2003, vol. 2, pp. 1648-1653 vol.2.

[17] G. S. Sawicki, C. L. Lewis, and D. P. Ferris, "It pays to have a spring in your step," *Exercise and sport sciences reviews,* vol. 37, no. 3, p. 130, 2009.

[18] K. E. Zelik and A. D. Kuo, "Human walking isn't all hard work: evidence of soft tissue contributions to energy dissipation and return," *The Journal of experimental biology,* vol. 213, no. 24, pp. 4257-4264, 2010.

[19] D. Winter, J. Eng, and M. Ischac, "Three-dimensional moments, powers and work in normal gait: implications for clinical assessments," in *Human motion analysis: current applications and future directions*, G. Harris and S. PA, Eds. New York: IEEE Press, 1996.

[20] D. J. Farris, B. D. Robertson, and G. S. Sawicki, "Elastic ankle exoskeletons reduce soleus muscle force but not work in human hopping," *Journal of Applied Physiology,* vol. 115, no. 5, pp. 579-585, 2013.

[21] J. Brockway, "Derivation of formulae used to calculate energy expenditure in man," *Human nutrition. Clinical nutrition,* vol. 41, no. 6, pp. 463-471, 1987.

[22] L. Hargrove, K. Englehart, and B. Hudgins, "The effect of electrode displacements on pattern recognition based myoelectric control," in *2006 International Conference of the IEEE Engineering in Medicine and Biology Society*, 2006, pp. 2203-2206.

[23] P. Kaufmann, K. Englehart, and M. Platzner, "Fluctuating emg signals: Investigating long-term effects of pattern matching algorithms," in *2010 Annual International Conference of the IEEE Engineering in Medicine and Biology*, 2010, pp. 6357-6360.